行政院國家科學委員會專題研究計畫　成果報告

奈米生醫複合材料之機械特性強化與藥物包覆及釋放之研究

計畫類別：個別型計畫
計畫編號：NSC93-2216-E-009-027-
執行期間：93 年 08 月 01 日至 94 年 07 月 31 日
執行單位：國立交通大學材料科學與工程學系(所)

計畫主持人：陳三元

報告類型：精簡報告
報告附件：出席國際會議研究心得報告及發表論文
處理方式：本計畫可公開查詢

中　華　民　國 94 年 8 月 24 日

奈米生醫複合材料之機械特性強化與藥物包覆及釋放之研究(I)

Effect of CDHA nanoparticles on drug release behavior of CDHA/Chitosan nanocomposites

奈米缺鈣磷灰石對於奈米複合材料之藥物釋放與特性研究

計畫編號：NSC-93-2216-E-009-027
執行時間：93/08/01 ~ 94/07/31

主持人：陳三元 教授　　交通大學材料科學與工程學系

中文摘要

本研究主要是在探討缺鈣型氫氧基磷灰石(Calcium-deficient Hydroxyapatite, CDHA)與幾丁聚醣(Chitosan, CS) 兩相摻和之無機-有機複合材料之物理性質與 B_{12} 藥物釋放滲透的行為。將鈣、磷與幾丁聚醣等前驅物，以不同添加順序為製程變數，結果顯示，以 in-situ 製備(磷酸溶液與幾丁聚醣先混合，最後加入醋酸鈣溶液)合成的 CDHA-CS 複合材料之滲透係數最低，可能因為 CDHA 與 CS 交聯程度高、CDHA 與 CS 界面最好、粒子小且均勻分散所造成的。以有機/無機比例為變數，隨著 CDHA 含量提高，使得交鏈程度上升，也導致孔隙度的提高。而使得 CS 含量 90% 時，滲透係數最低。

本研究中，發現製程中的磷酸根(PO_4^{3-})對交鏈程度產生之影響，會進而影響到滲透係數，且在 in-situ 合成過程中，CDHA 與 CS 基材的反應，可作為成核起始點，對於分散性有正面幫助，導致滲透係數下降，強度上升。奈米粒子與有機基材之界面反應，其對分子運動的影響，會對滲透產生重大的影響，而扮演界面橋樑的高分子電解質，不宜太少或太過。

關鍵字： 幾丁聚醣、缺鈣磷灰石、奈米複合材料、藥物釋放、交聯

Abstract

With the aim of the manipulation of release kinetics via bioactive nanofillers for orthopedic drug-loaded implants, the effect of CDHA nanofiller on drug release kinetics was studied by adopting vitamin B_{12} as a model drug from chitosan/Ca-deficient hydroxyapatite (CS/CDHA) nanocomposite membranes prepared in terms of different synthetic processes, i.e. in-situ and ex-situ routes, and various amounts of CDHA. A higher value of diffusion exponent (n) was obtained for the membranes in-situ synthesized compared to that ex-situ prepared. A well-fitted linear correlation between crosslink degree and n value indicates that drug diffusion across the membrane is controlled by the micro/nano-structure of the hybrid membrane, which is strongly influenced by both the synthesis process and the concentration of the nanofiller in the membrane. Permeability (P) of the membranes showed a lower value for those prepared via the in-situ process which is contributing to the higher crosslink degree and longer diffusion path. Furthermore, it was found that with increasing CDHA amount in the range below 10 wt%, the n value of in-situ CS/CDHA nanocomposite membranes increased but the P value decreased. However, as the CDHA content was increased more than 30%, an increased P value was observed but the n value remained constant.

Keywords: Chitosan, Ca-deficient hydroxyapatite, nanocomposite, drug release, crosslink

1. Introduction

Chitosan (CS) has been widely used as scaffolding materials in tissue engineering [1], orthopedic implants [2] and drug delivery vehicles [3] for many years because of its

outstanding

characters of such as osteoconductivity, biodegradability, and biocompatibility, and its low pricing. Nevertheless, chitosan is lack of sufficient mechanical strength, which restricts its uses for load-bearing applications, especially in orthopedics. Many studies have attempted to improve those properties by incorporating calcium phosphate bioactive ceramic such as hydroxyapatite (HAp, $Ca_{10}(PO_4)_6(OH)_2$) and , β-tricalcium phosphate (β-TCP, $Ca_3(PO_4)_2$) [4, 5]. However, natural bone mineral has essentially a calcium-deficient apatitic structure (Ca-deficient hydroxyapatite, CDHA) with a Ca/P ratio of about 1.5, which is compositionally similar to tricalcium phosphates (Ca/P = 1.5) and structurally similar to stoichiometric hydroxyapatite (Ca/P = 1.67). Therefore, CDHA is considered to be a candidate material with respect to both mechanical reinforcement and biological activity for orthopedic application.

The key successful point of macroporous scaffolding devices for osteogenesis is not only the suitable matrix with sufficient bioactivity and mechanical strength for osteogenic progenitor cells, but also the sustained release of antibiotic and growth factor to eliminate inflammation and insure osteoblast differentiation, respectively [3, 6]. Up to now, many studies have been done on the microstructure and mechanical properties of CS/HAp nanocomposites for orthopedic use [7, 8]. However, the role of CDHA nano-crystals in drug release behavior of chitosan-based composite has been barely found in the literature. Therefore, it is feasible to design a CS/CDHA nanocomposite as bone substitute loaded with bioactive agents with various release kinetics manipulated by the amount of CDHA nanofiller.

Generally, drug release kinetics of polymeric drug delivery system have been usually characterized by the use of membrane permeability (P) and diffusion exponent (n) which are used to describe the release behavior for membrane (reservoir) systems and the diffusion mechanism for matrix (monolithic) systems, respectively [9]. Furthermore, both indexes in polymer-based materials are strongly dependent on crystallinity, plasticization, glass transition temperature (T_g) and swelling of the polymer vehicle, which are also affected by the presence of nanofillers [10-12]. Most researchers found an increase in the T_g as a function of nanofiller content [13, 14]. On the contrary, a decrease in T_g with the increase of nanofiller was also reported [12, 15]. Furthermore, the influence of filler on resulting crystallinity of polymeric phase has been not consistently reported. Some reported that nanofiller acted as nucleation agent to enhance the crystallinity of semi-crystalline polymer [11]. However, some suggested that nanofiller could retard the evolution of crystalline structure within the polymeric domains of the composite [16]. These arguments are due to various extent of polymer-filler interaction in different composite systems [16, 17]. In order to classify the role of polymer-filler interaction in drug release behaviors of CS/CDHA nanocomposite, the in-situ preparation process was employed because this has been reported to improve the mechanical properties of chitosan/HAp composite through enhancing polymer-filler interaction [18].

In this work, with the aim of studying the roles of polymer-filler interaction in the drug release behavior of CS/CDHA nanocomposite, in-situ incorporation of the CDHA nanoparticles, i.e. CDHA synthesized in the presence of chitosan, was employed. For comparison, ex-situ synthetic process was also prepared. In other words, CDHA nanofiller was synthesized first and then added into the chitosan solution. Membrane permeability and diffusion exponent of CS/CDHA nanocomposites with various CDHA content were systematically investigated, aimed at exploring the influences of CDHA nanofillers on the drug release behavior and corresponding release mechanism.

2. Experimental Procedure

2.1. CS/CDHA nanocomposite membrane preparation

In this study, the CS/CDHA nanocomposite membranes with various CDHA content were prepared via in-situ and ex-situ process to characterize the influence of nanofiller and polymer-filler interaction on drug delivery behavior. CS with 215k molecular weight and 80% degree of deacetylation was supplied by Aldrich-Sigma. CS solution of 1%(w/v) was first prepared by dissolving CS powder in 10% (v/v) acetic acid solution. For ex-situ processes, CDHA nanoparticles were first synthesized by mixing $Ca(CH_3COO)_2$ aqueous solution with H_3PO_4 aqueous solution. The pH value was kept at 7.5 by the addition of NaOH solution (1M). The un-reacted precursors in the resulting CDHA suspension were removed by repeating precipitation and distilled-water (DI water) washing process for three times. The resulting CDHA/DI water suspension was added into CS solution to form CS/CDHA suspension. For in-situ process, H_3PO_4 aqueous solution (0.16M) was first added into CS solution and then $Ca(CH_3COO)_2$ aqueous solution (0.25M) was added into this mixture solution. The pH value was also kept at 7.5 by NaOH solution (1M). The composite membranes with the volume ratios of CS/CDHA controlled at 95/5, 90/10, 70/30 and 50/50 for both in-situ and ex-situ processes (see table I). Subsequently, those CS/CDHA suspensions were poured into Petri dish to form CS/CDHA membranes after drying at room temperature for 7 days.

2.2. Material characterization

The volume ratio of CS/CDHA was confirmed by thermogravitational analysis (TGA, Perkin Elmer). The Crystallographic phase of CS/CDHA composites were identified by X-ray diffractometer (XRD, M18XHF, Mac Science, Tokyo, Japan). The morphology of both composite membranes and CDHA nano-crystals was observed by using scanning electron microscopy (SEM, Hitachi S4000) and transmission electron microscopy (TEM, JEOL-2000FX).

2.3. Determination of diffusion exponent for drug-loaded matrix system

Vitamin B_{12} (Sigma, V-2876) is a water soluble agent with low molecular weight (1355Da), small molecular size and negligible interaction with CDHA, which is a suitable model drug for our system. It should be incorporated into CS/CDHA matrices in advance for diffusion exponent determination. The preparations of drug-loaded matrix membranes were similar to above mentioned process (section 2.1). Before membrane drying, vitamin B_{12} was added into those CS/CDHA suspensions. The subsequent drying process was also the same as above mentioned process (section 2.1). These composite membranes were put into PBS solution (phosphate-buffered solution, pH7.4) for release test. The release medium was withdrawn for each juncture and replaced with equivalent volume of fresh buffer. The released amount of vitamin B_{12} was determined by UV-visible spectroscopy (Agelent 8453) at 361 nm.

2.4. Determination of the permeability of membrane system

The permeation tests were performed by the use of side-by side diffusion cell. Vitamin B_{12} aqueous solution (90ml) of 0.02% (m/v) was added into the donor cell as model drug. The same volume of PBS solution was added into receptor cell. Drug-free composite membrane was fixed between the two half-cells. The amount of permeated vitamin B_{12} was determined by using UV-Visible spectroscopy for each juncture. The apparent partition coefficient (H) of vitamin B_{12} for CS-CDHA composite/aqueous medium was determined as follows [19]. Drug-free CS-CDHA composite (10 mg) was immersed in the release medium until equilibrium state. The wet weight (W) was recorded. The nanocomposite was then immersed in 10ml of vitamin B_{12}-containing medium. Partition coefficient (H) was determined from the initial (C_0) and equilibrium (C_e) concentration of vitamin B_{12}-containing mediums by using Eqn. 1:

$$H=10(C_0-C_e)/WC_e. \quad (1)$$

3. Results and Discussion

3.1 Material characterization

Figure 1 shows the cross-sectional area (fracture surface) of those composite membranes. For the in-situ process (Figure 1a, 1b and 1c), it can be found that most of the membranes showed non-porous with dimple-like fractured surface except for the In-situ 50 sample (Figure 1d), which is probably caused by plastic deformation. The number of dimple decreased and the dimple size increased as the CDHA content was increased. By contrast, for the ex-situ process, the membranes became porous when the CDHA amount was over 30% (Figure 1f). It is due to agglomeration of the incorporating CDHA nanoparticles, which are further evidenced by TEM as shown in Figure 2. These agglomerates could be the favorable sites for the nucleation of voids upon drying. Therefore, in this work, data of Ex-situ 30 and Ex-situ 50 were excluded due to their macro-porous structure, which could not comply with the fundamental hypothesis of Equations 1 and 2 in the forthcoming analysis [9].

Figure 3 shows the XRD patterns of CDHA, CS and CS/CDHA nanocomposites. One major peak at $2\theta\sim21^o$ and two minor peaks at $2\theta\sim26^o$ and 32^o appeared in both samples of In-situ 10 and Ex-situ 10. According to the ICDD No. 39-1894 and No. 46-0905, the major peak and two minor peaks can be identified as semi-crystalline chitosan and poorly crystalline CDHA, respectively. It indicated that CS/CDHA composites could be synthesized through both in-situ and ex-situ processes. Furthermore, it was found that the crystallinity of CS was decreased with increasing CDHA content, which is probably caused by the well-dispersed CDHA nano-crystals which act as point defect in the chitosan matrix [15]. As previously mentioned, the extent of CDHA agglomeration was increased as the CDHA content increased over 30%, which retarded crystallization. In addition, Strawhecker et al. also reported that strong polymer-filler interaction could change the molecular conformation of polymer chain in the vicinity of filler and simultaneously gave rise to the formation of localized amorphous regions [16]. This explains a considerable inhibition of the crystallinity development of chitosan crystals and this retard becomes more pronounced when the CDHA amount is greater than 30 wt%.

Figure 4 shows the TGA curves of CS/CDHA nanocomposite membranes prepared via the in-situ process. Thermal decomposition of pure chitosan without crosslink was clearly observed between 150^oC to 250^oC, which is attributed to the cleavage of hydrogen bonding [20]. The TGA curve of Ex-situ 10 was similar to that of In-situ 5 (not shown). However, no thermal decomposition region was observed for both In-situ 30 and In-situ 50 samples. Furthermore, it was found that as the pure chitosan membrane was fully crosslinked by TPP (tripolyphosphate), its TGA curve was very similar to that of both In-situ 30 and In-situ 50 samples. This result suggests that the CDHA act as a crosslinking medium with chitosan, which is attributed to the electrostatic attraction between $(PO_4)^{3-}$ moieties (from CDHA) and protonated amino groups (NH_3^+) in chitosan molecules. The electrostatic attraction force stabilizes polymer chain network via crosslinking operation. The degree of crosslink could be quantified by calculating the weight loss of the composite membranes with respect to the weight loss of pure chitosan in the range from 150^oC to 250^oC and the results are shown in Figure 5a. As can be seen, when the incorporated CDHA was below 10%, crosslink degree was almost linearly increased with CDHA content, above that, the correlation tended to become constant. This observation could be accounted for by assuming that all the NH_3^+ groups in chitosan molecules are fully occupied by interaction with the surface phosphate groups of the CDHA nanoparticles

and under such a full occupation, no further sites for crosslinking are available. On the other hand, for the sample with 10% of CDHA, the crosslink degree in the composite membranes prepared via the in-situ processes were higher than those prepared via the ex-situ alternative. It is then reasonably to believe that in-situ synthesis offers an overall stronger filler-polymer interaction and more CDHA nucleation site, thus making better dispersion of the CDHA nanoparticles in the chitosan matrix. In this condition, the well-dispersed CDHA nano-crystals provide more efficient crosslink with chitosan than that of the agglomerated CDHA nano-crystals prepared via the ex-situ process.

3.2 Diffusion exponent of drug-loaded matrix system

Diffusion exponent n, as defined in Eqn. (2), can be used to determine release kinetics and diffusion mechanism for polymeric matrix (monolithic) drug delivery systems (DDS). The values of n in Eqn. (2), for most polymeric DDS lie between 0.5 to 1 (anomalous diffusion) for the specimens with slab geometry. When the exponent n takes a value of 1.0, the drug release rate is independent of time (zero-order release kinetics). It indicates a swelling controlled mechanism (Case II transport). For n=0.5, it indicates diffusion controlled mechanism (i.e., Fickian diffusion). The diffusion exponent n of non-porous materials can then be determined by the use of Power Law [21, 22]:

$$(M_t/M_\infty) = kt^n \qquad (2)$$

where M_t is the amount of drug released at time t, M_∞ is the amount of drug released at equilibrium state, k is a constant and n is diffusion exponent related to the diffusion mechanism. As revealed in Figure 5a, the exponent n was strongly affected by synthetic process and concentration of the nanofiller. It was observed that the n values of the membranes synthesized through in-situ processes were higher than those through ex-situ process. This, according to previous argument, is probably due to the stronger polymer-filler interaction between CS and well-dispersed CDHA crystals, and higher crosslink degree particularly for the in-situ route. This assumption is further supported by DMTA curves shown in Figure 6. It is known that for semi-crystalline polymers, short range interaction in side-chain such as polymer-filler interaction causes a shift of β-transition to higher temperature region. Long range interaction in backbone causes an α-transition broadened or even peak disappeared [11-12, 15]. These two phenomena were both observed in the DMTA curves for sample In-situ 10. It suggests that well-dispersed CDHA nanoparticles, i.e., in-situ route, provide greater extent of crosslink with the chitosan and more effectively reduce the molecular relaxation rate of chitosan molecules, i.e., restricted relaxation. This restriction of molecular relaxation is believed to equivalently affect drug diffusion within the nanocomposites and result in an increase of exponent n, indicating that drug release shifts from diffusion-controlled towards swelling controlled mechanism [22].

Hongbin et al. reported a coarse-grained domain relaxation model to depict the restricted relaxation behavior in the nanocomposite system based on the nature of polymer-filler interaction [14]. The polymer chains around filler can be classified into three regions: Domain I (slow relaxation region in the vicinity of filler), Domain II (fast relaxation region in the central areas among neighboring fillers), and Domain III (normal relaxation region in bulk matrix). This model supports α-transition peak observed in sample Ex-situ 10. It is due to poor dispersion of CDHA nanofillers in the CS matrix, which increases the areas of Domain III. Therefore, restricted molecular relaxation in the membrane prepared via the ex-situ process is not as prominent as that prepared via the in-situ process. Therefore, the diffusion exponent of the CS/CDHA membranes is lower for the ex-situ

processes than that through the in-situ synthesis, as further confirmed in Figure 5a.

The effect of CDHA content on diffusion exponent is illustrated in Figure 5a. For pure CS, n was close to 0.5, indicating a Fickian diffusion kinetics. Incorporating the CDHA nanoparticles into CS matrices caused an increased n, which is well explainable in terms of the coarse-grained domain relaxation model. Increasing the concentration of the CDHA gives rise to an increase in polymer-filler interaction, leading to an increased volume of Domain I, and at the same time, reduces the volume of Domain II and Domain III. This indicates that the extent of restricted relaxation is increased as the concentration of CDHA increases. Therefore, when the CDHA was added up to 10%, exponent n was rapidly increased to 0.7 for the nanocomposite prepared via the in-situ process, indicating a transition from diffusion control to swelling control. Furthermore, from experimental findings, when the CDHA was increased from 10% to 30%, the volume for Domain II and III were largely replaced by Domain I and tended to approach a saturated level. The n value then became relatively constant when the CDHA content was over 30%. Interestingly, this phenomenon reveals that the effect of CDHA content on diffusion exponent n is very similar to that of CDHA content on crosslink degree. This also implies a possible correlation of diffusion exponent with the degree of crosslink. Figure 5b shows the resulting dependence, where a linear correlation with R^2 as high as 0.98 was obtained. It indicates that the degree of crosslink within the matrix due to the incorporation of CDHA nanoparticle profoundly affects the drug diffusion exponent. However, it is believed that the factors such as the orderliness of the matrix (i.e., crystallinity) and the distribution of the CDHA nano-phase (i.e., connectivity) acting as a physical barrier for drug diffusion also influences the resulting diffusion exponent. It is more interesting if those factors can be clearly differentiated in terms of respecting contribution on the drug diffusion or more practically, drug release behavior. However, difficulty will also arise since some of factors are highly inter-related, especially when the matrix chitosan phase interacted with the CDHA nano-phase, and hardly clearly separated. Therefore, although no definitive conclusion can be drawn at current stage, to the first approximation, it is believed that the linear correlation in Figure 5b exists and such correlation is essentially an intrinsic nature of the CS/CDHA nanocomposites.

3.3 Permeability of membrane system

Membrane permeability of polymeric film can be determined based on Eqn. (3) [23]:

$$\text{Ln}\,(1-C_t/C_0) = -(2ADH/V) = -(2AP/V) \qquad (3)$$

where C_t is the solution concentration in the receptor cell at time t, C_0 is the initial solute concentration of the donor cell, V is the volume of each half-cell, A is the effective area of permeation, D is diffusion coefficient, H is partition coefficient, and P is membrane permeability (P = D*H). The slope of the plot of $-((V/2A)\,\text{Ln}\,(1-C_t/C_0))$ versus t is membrane permeability. The effect of CDHA content on the permeability and partition coefficient of the membrane prepared through the in-situ process is illustrated in Figure 7. It was found that the partition coefficient was slightly decreased with increasing CDHA content because the incorporated CDHA do not dissolve model drug. It suggests that the diffusion coefficient (D) becomes the dominant item for the membrane permeability (P=D*H). The membrane permeability was decreased with the incorporation of CDHA from 0% to 10%. However, further increase in the CDHA from 10 to 30% caused an increase in the permeability which became more pronounced when the CDHA content was greater than 30%. The extent of crosslink and the length of diffusion path increase with the incorporation of CDHA nanofillers, leading to the decrease of diffusion

coefficient. Therefore, the membrane permeability of CS/CDHA nanocomposite decreased with increasing CDHA content. On the contrary, the crystallinity decreased as the CDHA was incorporated into the chitosan matrix as evidenced in Figure 3. The CDHA nanoparticles retard the crystallization of chitosan, thus making the resulting chitosan more amorphous, which in turn increases the diffusion coefficient of the chitosan matrix [24]. Therefore, the influence of the CDHA on the chitosan diffusion coefficient is essentially a compromise between crosslink degree and crystallinity. As the CDHA content was increased over 30%, the decrease in the crystallinity of the chitosan became dominant. In addition, a further addition of CDHA causes agglomeration between the nanoparticles as observed in sample In-situ 50 which may further induce the formation of the microcracks between the CDHA phase and chitosan matrix as a result of increased rigidity or more specifically, voids within the CDHA agglomerates. Either microcracks or voids could act as effective paths, which causes a significant increase in permeability, as observed in sample In-situ 50%.

Figure 7 also shows the influence of synthetic processes on membrane permeability. For the CDHA content of 5% and 10%, the permeability of composite membranes was lower for the in-situ route than that via ex-situ process. This is probably due to better dispersion of the CDHA nanoparticles for samples prepared by in-situ process, resulting in more efficient physical barriers. A higher degree of the crosslink (Figure.5a), compared to the ex-situ synthesis, also provides inhibition to the resulting diffusion coefficient.

Based on aforementioned argument, it is desired to manipulate the release profile by selecting suitable values of n and P through incorporating various CDHA. Taking 5%, 30% and 50% as examples, the resulting drug release profiles for vitamin B_{12} from matrix membranes are illustrated in Figure 8. A near-zero order release profile with rapid release rate was observed for 50% (In-situ 50) matrix membrane samples (with n=0.72, P=8.9 * 10^{-4} cm^2/h, H=0.096, D=9.3 * 10^{-3} cm^2/h); however, a near-zero order release profile with moderate release rate was achieved for 30% case (with n=0.71, P=3.4 * 10^{-4} cm^2/h, H=0.103, D=3.5 * 10^{-3} cm^2/h). It suggests that D value could be altered drastically without changing n value in the range of CDHA amount from 30% to 50%. Compared with In-situ 30, a relative long-term release was achieved for In-situ 5 sample (with n=0.6, P=3.7 * 10^{-4} cm^2/h, H=0.112, D=3.7 * 10^{-3} cm^2/h), whose D value was close to that of In-situ 30.

Recently, sequential release of growth factor has been reported because of its potential to enhance wound healing and osteogenesis [25]. In addition, using combination antibiotic therapy to decrease antibiotic-resistance has been investigated [26, 27]. Unfortunately, the effect of different bioactive agents or drugs may be therapeutically inconsistent or possibly adversely interacted in the same carrier materials. In order to synergize the therapeutical efficacy of multiple bioactive agents, it is more clinically desirable to precisely manipulate drug release profiles either simultaneously or sequentially. Adapting biodegradable polymeric microspheres reinforced by Ca phosphate to fill bone defect has been pursed to achieve satisfactory results [28]. Therefore, it is feasible to design a bone filler loaded with multiple drugs for simultaneous release or sequential release profile via using CS/CDHA composite microspheres with various release kinetics regulated by the amount of CDHA nano-phase. Compared with existing conventional approaches with various drug release kinetics (i.e., molecular weight, crystallinity, amount of crosslink agent), this study provides a relatively simple, precise and controllable synthetic methodology to manipulate release kinetics based solely on both the chitosan and CDHA as starting precursors.

4. Concluding Remarks

In conclusion, an orthopedic implant material made of chitosan and CDHA with drug delivery function has been studied. It was found that both incorporated CDHA amount and synthetic process significantly altered the drug release behaviors of CDHA/chitosan nanocomposites. Moreover, the manipulation of diffusion exponent and permeability could be achieved by simply regulating the amount of CDHA nanocrystal acting as bioactive nanofiller and release regulator, which may provide valuable information for a better design of chitosan-based orthopedic devices with improved bioactivity and controlled drug release function.

Acknowledgement

The authors gratefully acknowledge the National Science Council of the Republic of China for its financial support through Contract No. NSC-93-2216-E-009-027.

References

1. Zhao F, Yin Y, Lu WW, Leong JC, Zhang W, Zhang J, Zhang M, Yao K, Preparation and histological evaluation of biomimetic three-dimensional hydroxyapatite/chitosan–gelatin network composite scaffolds, Biomaterials 23 (2002) 3227-3234.
2. G. S. Sailaja, S. Velayudhan, M. C. Sunny, K. Sreenivasan, H. K. Varma, P. Ramesh, Hydroxyapatite filled chitosan-polyacrylic acid polyelectrolyte complexes, J. Mater. Sci. 38 (2003) 3653-3662.
3. Ahn JS, Choi HK, Chun MK, Ryu JM, Jung JH, Kim YU, Cho CS, Release of triamcinolone acetonide from mucoadhesive polymer composed of chitosan and poly(acrylic acid) in vitro, Biomaterials 23 (2002) 1411-1416.
4. Michio Ito, Yuichi Hidaka, Mituharu Nakajima, Hiroshi Yagasaki, A. H. Kafrawy, Effect of hydroxyapatite content on physical properties and connective tissue reactions to a chitosan–hydroxyapatite composite membrane, J. Biomed. Mater. Res. 45 (1999) 204-208.
5. Yin YJ, Ye F, Cui JF, Zhang FJ, Li XL, Yao KD, Preparation and characterization of macroporous chitosan-gelatin beta-tricalcium phosphate composite scaffolds for bone tissue engineering, J. Biomed. Mater. Res. A 67 (2003) 844-855.
6. M. Geiger, R.H. Li, W. Friess, Collagen sponges for bone regeneration with rhBMP-2, Adv. Drug. Deliver. Rev. 55 (2003) 1613-1629.
7. Fei Chen, Zhou-Cheng Wang, Chang-Jian Lin, Preparation and characterization of nano-sized hydroxyapatite particles and hydroxyapatite/chitosan nano-composite for use in biomedical materials, Mater. Lett. 57 (2002) 858-861.
8. Isamu Yamaguchi, Shunsuke Iizuka, Akiyoshi Osaka, Hideki Monmad, Junzo Tanaka, The effect of citric acid addition on chitosan/hydroxyapatite composites, Colloid Surf. A-Physicochem. Eng. Asp. 214 (2003) 111-118.
9. R. Langer, Polymeric delivery system for controlled drug release, Chem. Eng. Commun. 6 (1980) 1-48.
10. L. H. Sperling, Introduction to physical polymer science, Second edition, John Wiley & Sons, New York, 1992, pp. 148-149.
11. Kesenci K, Fambri L, Migliaresi C, Piskin E, Preparation and properties of poly(L-lactide)/hydroxyapatite composites, J. Biomat. Sci-Polym. E. 11 (2000) 617-632.
12. V. Arrighi, I.J. McEwen, H. Qian, M.B. Serrano Prieto, The glass transition and interfacial layer in styrene-butadiene rubber containing silica nanofiller, Polymer 44 (2003) 6259-6266.
13. H.W. Goh, S.H. Goh, G.Q. Xu, K.P. Pramoda, W.D. Zhang, Dynamic mechanical behavior of in situ functionalized multi-walled carbon nanotube/phenoxy resin composite, Chem. Phys. Lett. 373 (2003)

277-283.
14. Hongbin Lu, Steven Nutt, Restricted relaxation in polymer nanocomposites near the glass transition, Macromolecules 36 (2003) 4010-4016.
15. Yu Qiang Huang, Yan Qi Zhang, You Qing Hua, Studies on dynamic mechanical and rheological properties of LLDPE/nano-SiO2 composites, J. Mater. Sci. Lett. 22 (2003) 997-998.
16. K. E. Strawhecker, E. Manias, Crystallization behavior of poly(ethylene oxide) in the presence of Na^+ montmorillonite fillers, Chem. Mater. 15 (2003) 844-849.
17. B.J. Ash, L.S. Schadler, R.W. Siegel, Glass transition behavior of alumina/polymethylmethacrylate nanocomposites, Mater. Lett. 55 (2002) 83-87.
18. Qiaoling Hu, Baoqiang Li, Mang Wang, Jiacong Shen, Preparation and characterization of biodegradable chitosan/hydroxyapatite nanocomposite rods via in situ hybridization: a potential material as internal fixation of bone fracture, Biomaterials 25 (2004) 779-785.
19. Makoto Miyajima, Akiko Koshika, Jun'ichi Okada, Masaru Ikeda, Mechanism of drug release from poly(L-lactic acid) matrix containing acidic or neutral drugs, J. Control. Release 60 (1999) 199-209.
20. Canh Le Tien, Monique Lacroix, Pompilia Ispas-Szabo, Mircea-Alexandru Mateescu, N-acylated chitosan: hydrophobic matrices for controlled drug release, J. Control. Release 93 (2003) 1-13.
21. N.A. Peppas, Analysis of Fickian and non-Fickian drug release from polymers, Pharm. Acta. Helv. 60 (1985) 110-111.
22. N.A. Peppas, R.W. Korsmeyer, Dynamically swelling hydrogels in controlled release applications, in: N.A. Peppas (Ed.), Hydrogels in Medicine and Pharmacy, Vol. 3, CRC Press, Boca Raton, 1986, pp. 109-136.
23. NA Peppas, NM Franson, The swelling interface number as a criterion for prediction of diffusional solute release mechanism in swellable polymers, J. Appl. Polym. Sci. 21 (1983) 983-997.
24. Seo J, Han H, Water diffusion studies in polyimide thin films, J. Appl. Polym. Sci. 82 (2001) 731-737.
25. A.T. Raiche, D.A. Puleo, In vitro effects of combined and sequential delivery of two bone growth factors, Biomaterials 25 (2004) 677–685.
26. Tatman-Otkun M, Gurcan S, Ozer B, Shokrylanbaran N, Annual trends in antibiotic resistance of nosocomial Acinetobacter baumannii strains and the effect of synergistic antibiotic combinations, Microbiologica 27 (2004) 21-28.
27. Miller YW, Eady EA, Lacey RW, Cove JH, Joanes DN, Cunliffe WJ, Sequential antibiotic therapy for acne promotes the carriage of resistant staphylococci on the skin of contacts, J. Antimicrob. Chemother. 38 (1996) 829-837.
28. M. Borden, S.F. El-Amin, M. Attawia, C.T. Laurencin, Structural and human cellular assessment of a novel microsphere-based tissue engineered scaffold for bone repair, Biomaterials 24 (2003) 597–609

.

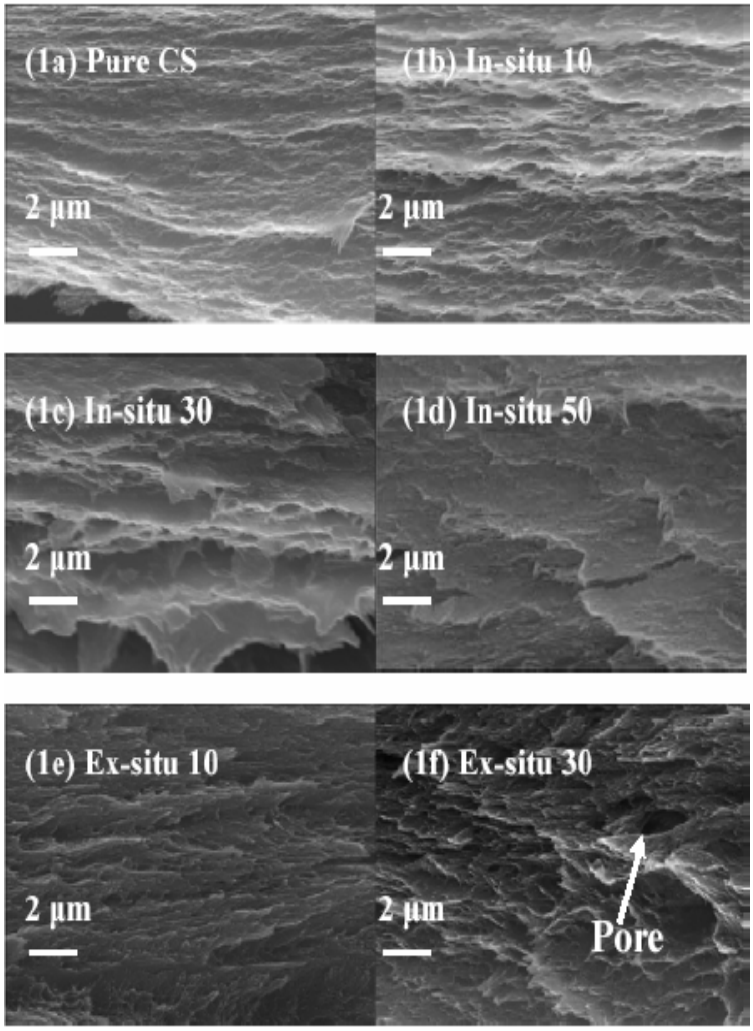

Fig. 1 Selective SEM micrographs (cross section) of CS/CDHA nanocomposite membranes.

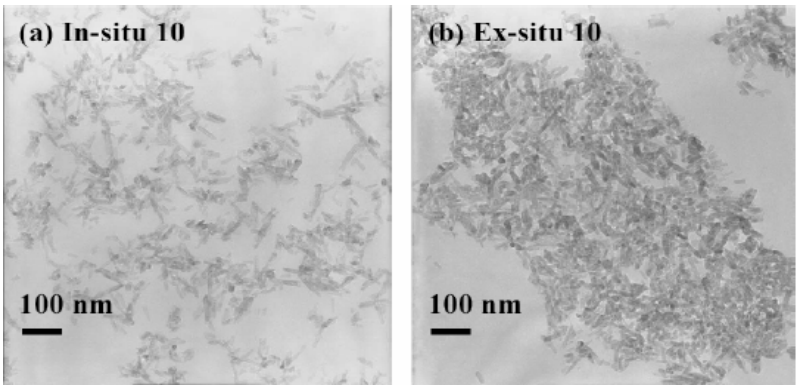

Fig. 2. Selective TEM micrographs of CS/CDHA nanocomposite membranes.

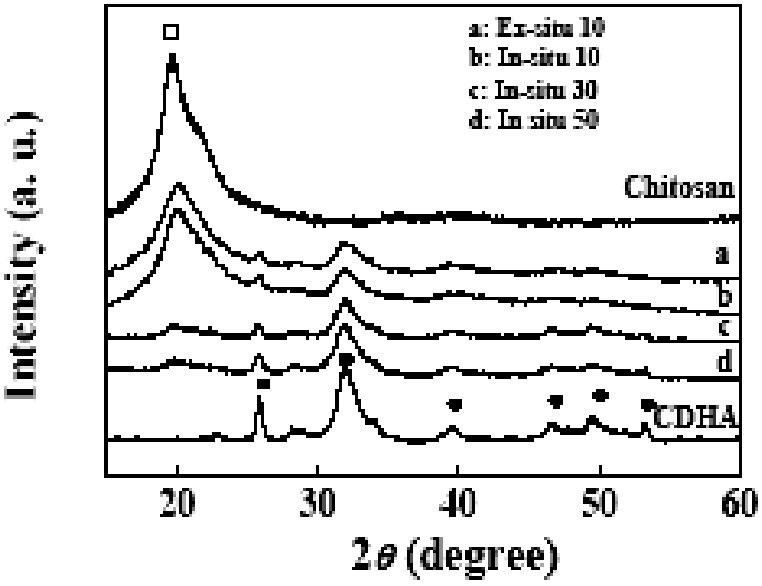

Fig. 3. XRD patterns of CS, CDHA and CS/CDHA nanocomposites.

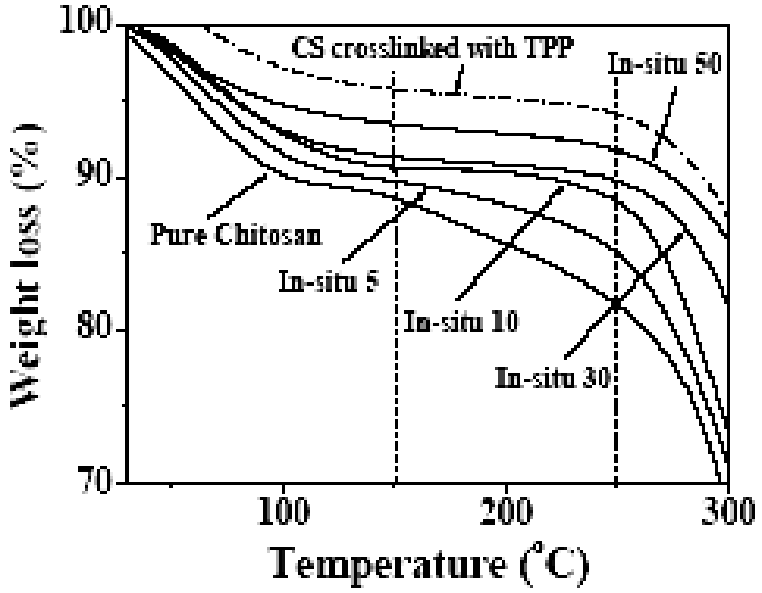

Fig. 4. TGA curves of TPP-crosslinked chitosan and CS/CDHA nanocomposite membranes prepared via in-situ process.

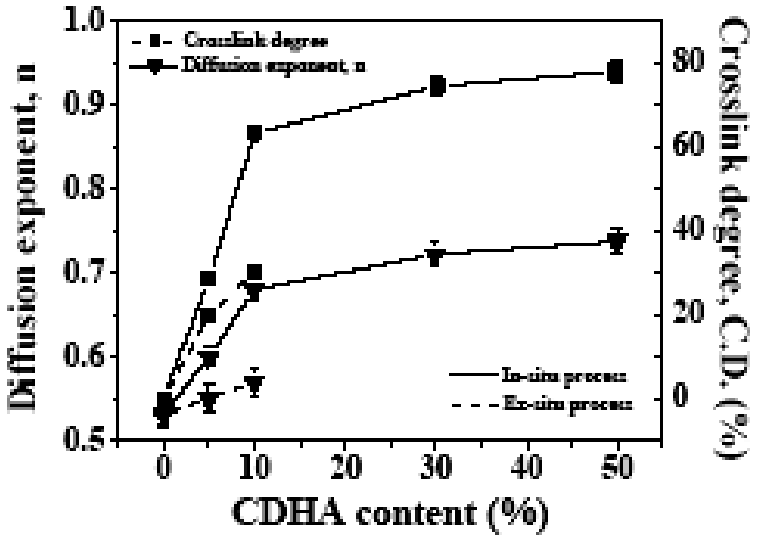

Fig. 5a. Dependences of synthetic processes and CDHA amount on the crosslink degree and diffusion exponent of nanocomposite membranes.

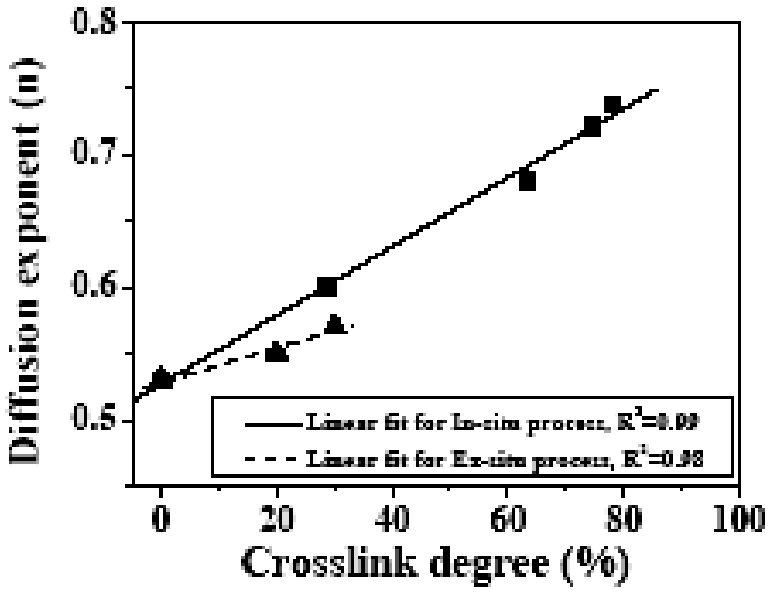

Fig. 5b. Dependences of crosslink degree on the diffusion exponents of nanocomposite membranes.

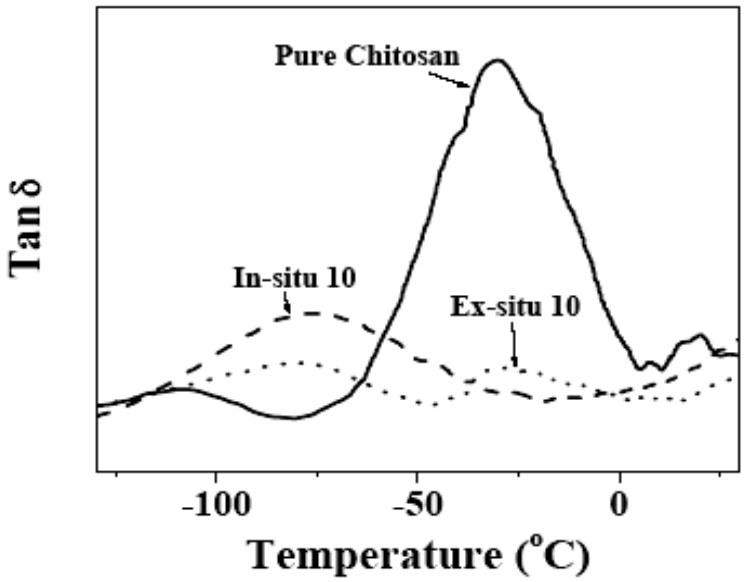

Fig. 6. DMTA curves of chitosan and CS/CDHA nanocomposite membranes with CDHA content 10%.

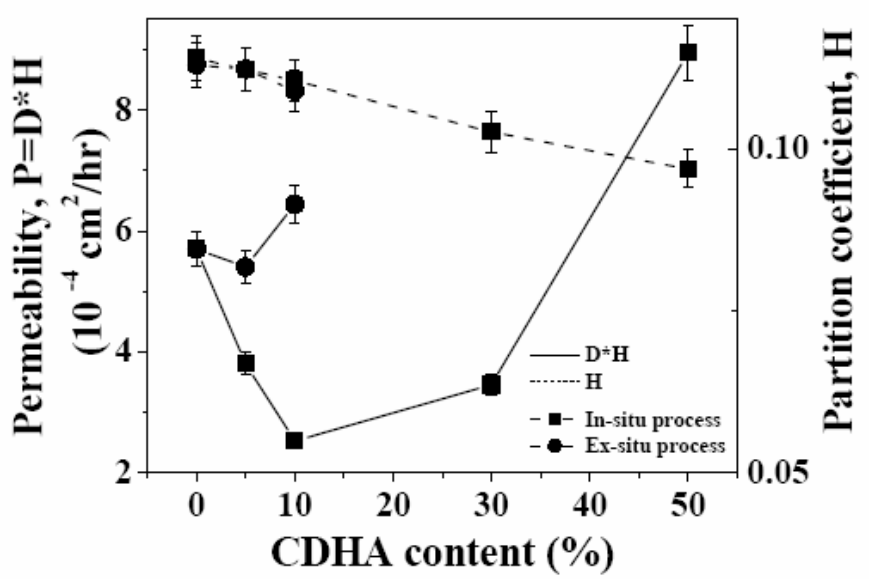

Fig. 7. Dependences of synthetic processes and CDHA content on the permeability (P) and partition coefficient (H) of CS/CDHA nanocomposite membranes.

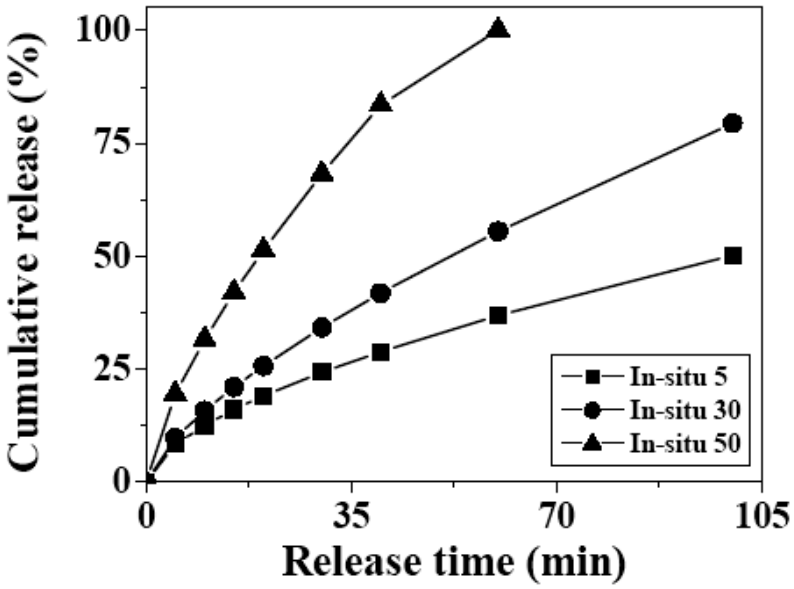

Fig. 8. Release profiles of CS/CDHA nanocomposite matrix membranes